Principal Component Analysis for Computation of the Magnetization Characteristics of Synchronous Reluctance Machine

Maria Nutu, Horia F. Pop
Department of Computer Science
Babeş - Bolyai University
Cluj - Napoca, Romania
Email: maria.nutu@cs.ubbcluj.ro

Radu Martis, Clauda Martis
Department of Electrical Machines and Drives
Technical University of Cluj-Napoca
Cluj - Napoca, Romania
Email: radu.martis@emd.utcluj.ro

***Abstract*—This paper is intended to bring added value in the interdisciplinary domains of computer science and engineering, in particular, electrical machines and machine learning. We present two approaches - Principal Component Analysis and Polynomial Interpolation to reduce the dimensions for the families of d- and q- axis currents curves, which describe the magnetostatic characteristics of a Synchronous Reluctance Machine (SynRM).**

***Keywords*—Principal Component Analysis, Polynomial Interpolation Methods, Synchronous Reluctance Machine**

I. Introduction

The intensive works in optimal design and analysis during the last decade have made of Synchronous Reluctance Machine (SynRM) a viable and competitive candidate of induction machine in medium and low power applications [1]–[4]. With no magnets and low rotor losses, rather low torque ripple, noise and vibrations, as well as simple and robust structure, SynRM is considered also for a wide variety of applications requiring variable speed operation in a large speed range, including field weakening [5]–[9].

The evaluation of Synchronous Reluctance Machine (SynRM) performances and of its dynamic response requires advanced models, to better account for the nonlinear behavior of the machine, including iron losses, saturation and cross-saturation. Moreover, control performances, especially in sensorless operation, are sensitive to estimation of machine parameters (resistance and direct and quadrature axis inductances). The influence of these phenomena on parameters estimation was presented and analyzed in several research works [10]–[12], and different models were proposed, developed and tested over the years [13]–[15]

Saturation and cross-saturation effects cannot thus be ignored and need to be integrated in the modeling of the SynRM. Therefore an accurate computation of the direct (d-) and quadrature (q-) inductances or flux linkages is required. Different theoretical and experimental methods (machine characterization procedures) were proposed, most of them addressing the computation of d- and q-axis inductances or flux linkages versus current(s)/rotor position maps. But, regardless of the type of the procedure, it demands time consuming tests and/or simulation.

The present paper proposes a simple method to build the d- and q-flux linkage maps by estimating an orthogonal basis for the multidimensional space spanned by the family of curves describing the magnetic characteristics of a SynRM. The family of curves results from Finite Element Analysis (FEA) applied to a SynRM topology, but it can be also the result of experimental measurements. Section II of the paper describes the machine under study and its mathematical model, emphasizing the role played by the d- and q- inductances in SynRM design and performances. Section III presents the Principal Component Analysis theoretical background and Section IV explains its implementation for SynRM d- and q-axis flux linkage versus currents/rotor position maps. In section V linear and spline interpolation methods are applied as an alternative to PCA for solving dimensionality reduction problem. Conclusions and perspectives are included in Section VI.

II. ELECTRICAL MACHINE MODEL

The equations defining the behavior of SynRM in rotor dq-coordinates are as follows:

$$u_d = R_s i_d + \frac{\partial \Psi_d}{\partial t} - \omega \Psi_q \tag{1}$$

$$u_q = R_s i_q + \frac{\partial \Psi_q}{\partial t} - \omega \Psi_d \tag{2}$$

$$T = \frac{3}{2} p (\Psi_d i_q - \Psi_q i_d) \tag{3}$$

$$T = J \frac{\mathrm{d}\Omega}{\mathrm{d}t} + B\Omega + T_{load} \tag{4}$$

The model is generally developed based on the assumption that the flux distribution is sinusoidal and, in a first approximation, for a SynRM, the d- and q-axis flux linkages can be written as:

$$\begin{aligned} \Psi_d &= L_d i_d \\ \Psi_q &= L_q i_q \end{aligned} \tag{5}$$

Substituting (5) into (1) and (2) and rearranging them:

$$\frac{\partial i_d}{\partial t} = \frac{1}{L_d}(u_d - R_s i_d + \omega L_q i_q) \tag{6}$$

$$\frac{\partial i_q}{\partial t} = \frac{1}{L_q}(u_q - R_s i_q + \omega L_d i_d) \tag{7}$$

The electromagnetic torque results as:

$$T = \frac{3}{2} p (L_d - L_q) i_q i_d \tag{8}$$

Moreover, the maximum power factor is given by:

$$\cos \phi_{max} = \frac{\frac{L_d}{L_q} - 1}{\frac{L_d}{L_q} + 1} = \frac{\varsigma - 1}{\varsigma + 1} \tag{9}$$

Thus, the machine is completely defined and its performances can be evaluated once the L_d and L_q values are available. The analytical computation of the inductances is difficult due to the different saturation degrees of the rotor core and to the complex path of d- and q-axis flux. A more accurate, but higher time and resources consuming computation of L_d and L_q can be done by using Finite Element (FE) based analysis (See Fig. 1 and Fig. 2). The model of the machine is implemented in a FE-based software package and the magnetostatic analysis is done at different rotor positions and for different i_d and i_q currents, obtaining the d- and q-axis magnetization characteristics of the machine. The d- and q-axis flux linkages as a function of rotor position and d- and q-axis currents, respectively for a SynRM with the cross-section presented in Fig.1 are depicted in Fig.2

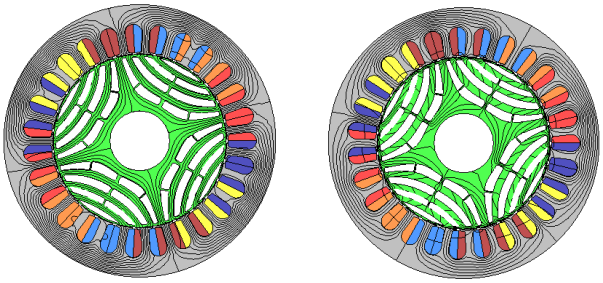

Fig. 1: Cross-section and d- and q-axis flux lines for a SynRM

Direct and quadrature inductances L_d and L_q can be then computed as derivative of flux linkage with respect to current i_d and i_q:

$$L_d = \frac{\mathrm{d}\Psi_d}{\mathrm{d}i_d}\Big|_{i_q=cst} \approx \frac{\Delta\Psi_d}{\Delta i_d}\Big|_{i_q=cst} \tag{10}$$

$$L_q = \frac{\mathrm{d}\Psi_q}{\mathrm{d}i_q}\Big|_{i_d=cst} \approx \frac{\Delta\Psi_q}{\Delta i_q}\Big|_{i_d=cst} \tag{11}$$

In order to reduce the d- and q-axis flux computing time the identification of the minimum number of simulation/measurement operation points is necessary, each operation point being defined by a d- and a q-axis current.

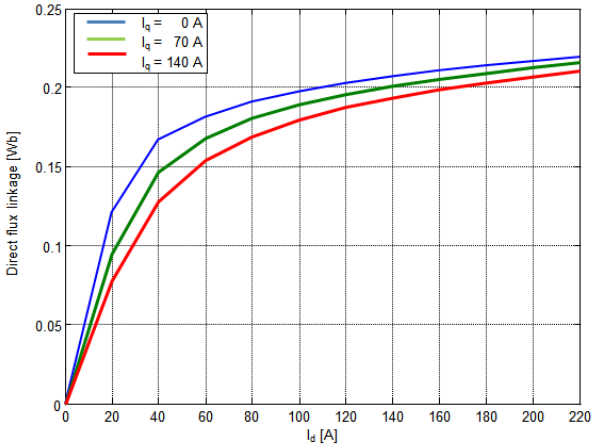

(a)

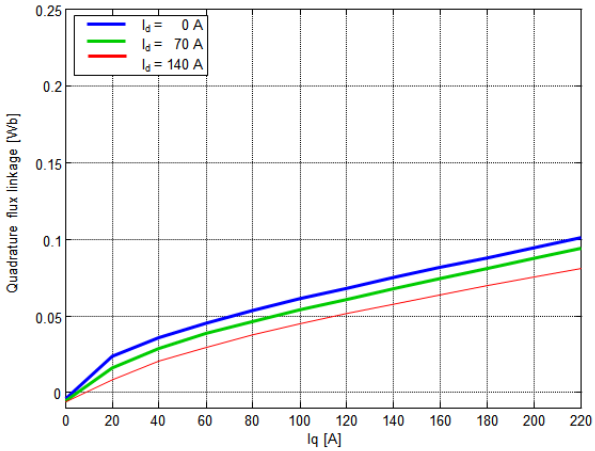

(b)

Fig. 2: d- and q-axis flux linkage as function of d- and q-axis currents

III. PRINCIPAL COMPONENT ANALYSIS - THEORETICAL BACKGROUND

Principal Component Analysis (PCA) is an unsupervised learning method used for linear dimensionality reduction. PCA finds new fewer linearly independent properties, which can project the original data into a reduced space, with a minimal loss of information [16], [17]. These new properties, called Principal Components (PCs), are linear combinations of the initial data features. PCs are ranked based on the variance of data contained in it. In the statistics field, "variance" is synonym with "more information". This means that the second PC retains less data that the first PC, but more than the third one. The number of PCs is equal to the number of the data features. In order to obtain a reduced space, only those PCs which capture enough variance will be retained. These should predict or reconstruct the data in the original dimensions, with a minimized error (in terms of least mean squared error). In this paper, PCs are computed based on Singular Value Decomposition (SVD) of the data. Both PCA

and SVD are linear techniques. This implies the use of linear transformations of data. In order to ease data manipulation, it will be represented in matrix form, being known that matrix multiplication easily express rotation, scaling, reflection, skew or linear operations, in terms of linear algebra.

A. Singular Value Decomposition

In linear algebra, using SVD factorization, any $m \times n$ matrix X can be expressed as a product of three matrices [18]

$$X = U\Sigma V^t \tag{12}$$

where U is a $m \times m$ orthogonal matrix ($UU^t = I_{m\times m}$); Σ is a $m \times n$ diagonal matrix; V^t is a $n \times n$ orthogonal matrix ($VV^t = I_{n\times n}$); V^t = transpose of matrix V.The columns of matrix U are called *left singular vectors* and form an orthonormal basis for the columns of X - for the features space. This means:

$$u_i u_j = \begin{cases} 1, & i = j \\ 0, & i \neq j \end{cases} \tag{13}$$

The rows of matrix V^t are called *right singular vectors* and form an orthonormal basis for the rows of X - for the samples space. The elements of Σ are nonzero on the main diagonal, and zero otherwise. The nonzero elements are called *singular values*, and, by convention, are in descending order, with the highest element in the upper-left corner of the matrix.

To obtain the SVD for a $m \times n$ matrix X:

- Compute X^t and XX^t
- Compute the eigenvalues λ of $A = XX^t$, using the *characteristic equation*:

$$\det(A - \lambda I) = 0 \tag{14}$$

- Sort them in descending order and compute their square roots, which will be the singular values of X.
- Complete the Σ matrix with X singular values. Compute its inverse, Σ^{-1}.
- With the λ values from above, compute the eigenvectors for $A^t = X^T X$. Complete the matrix V with these eigenvectors and transpose it, in order to obtain V^t.
- Compute $U = XV\Sigma^{-1}$
- To complete the SVD, write $X = U\Sigma V^t$

B. Covariance Matrix

In order to express the correlation between two features, the covariance matrix C will be computed. It is a symmetric matrix with:

- Variance of the variables along the main diagonal

$$var(x) = \frac{1}{n-1}\sum_{i=1}^{n}(x_i - \bar{x})^2 \tag{15}$$

- Covariance between each pair of variables in the left positions.

$$var(x, y) = \frac{1}{n-1}\sum_{i=1}^{n}(x_i - \bar{x})(y_i - \bar{y}) \tag{16}$$

where $\bar{x}$ is the mean of sample x.

The variance of data expresses how spread the data set is, while the covariance measure the extent to which two random variables x, y, vary together.

C. SVD, Covariance matrix and PCA

PCA's goal is to find new independent axis on which the projected data has maximal variances. Moreover, covariance among those new dimensions should be 0, so the resulting data will be uncorrelated, which leads to linearly independent directions. In mathematical terms, this means a diagonal covariance matrix.

From Spectral Theorem of linear algebra [19], [20], a symmetric matrix is diagonal in its eigenvector basis. Thus, the principal components are, in fact, the eigenvectors of the Covariance matrix. PCA gives optimal results if data are mean centered (each sample has zero-mean). This implies that covariance matrix becomes $C = XX^t$.

To sum up, PCA main steps are [21], [17]:

- Arrange data as a $m \times n$ matrix, where m is the number of samples and n is the number of features or measurements.
- Mean center the data
- Apply SVD on the covariance matrix (to obtain a diagonal representation)
- PCs are the eigenvectors of the covariance matrix. Choose only the first k PCs (k = dimension of the reduced projection space).

IV. PCA APPLIED ON SYNRM D - AXIS FLUX LINKAGE VERSUS CURRENTS

The algorithm was implemented in Python. The dataset set was organized as a matrix of d-axis flux linkage versus currents. d- and q-axis currents have values between 0 and $220A$. The original graphical representation for all the 12 I_q curves is captured in Fig3

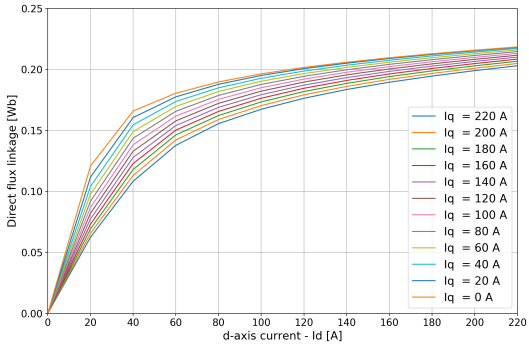

Fig. 3: Original Plots for I_q currents

A. Reducing the number of I_q curves

The first PCA implementation aims to reduce the number of I_q curves used to describe the d-axis flux linkage. We tried to

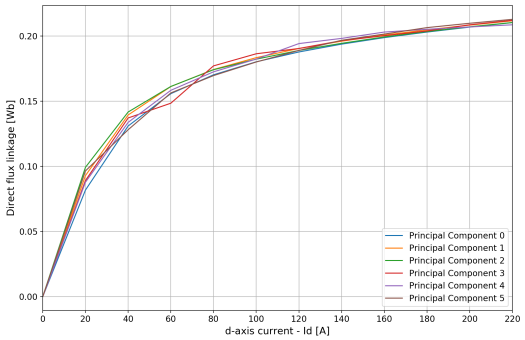

Fig. 4: Top 6 Principal Components

reduce the 12 initial samples, considered to be 12 dimensions in terms of PCA, to 2, 4 and 6 PCs (see Fig. 4)

The average weights of I_q curves in each PCA case study are listed in Table I

I_q values	Number of PCs		
	2	4	6
220 A	0.6	0.4	0.3
200 A	0.3	0.4	0.3
180 A	0.2	0.2	0.2
160 A	0.2	0.3	0.3
140 A	0.2	0.2	0.2
120 A	0.2	0.2	0.2
100 A	0.2	0.1	0.2
80 A	0.2	0.1	0.2
60 A	0.1	0.1	0.2
40 A	0.1	0.2	0.2
20 A	0.2	0.1	0.2
0 A	0.2	0.2	0.2

TABLE I: Average weights of I_q

A Ridge regression model [22] was trained in order to predict the I_q value for each of the 6 PCs (Table II).

Principal Component 0	129.0 A
Principal Component 1	107.0 A
Principal Component 2	110.0 A
Principal Component 3	110.0 A
Principal Component 4	110.0 A
Principal Component 5	110.0 A

TABLE II: Principal Components predicted values (I_q values)

The predicted values range is from 107 A to 129 A, with the same value for the last four PCs. As mentioned before, the most important information is concentrated in the first PCs, in descending order. This being observed, we can conclude the first three PCs are sufficient to reconstruct the family of all 12 I_q curves, obtaining the d-axis magnetization characteristics of the SynRM. This result efficiently enables us to cut the problem dimensionality by quarter (from 12 samples measurements to only 3 samples), with an $10^(-6)$ order error, leading to fewer tests and/or simulations.

B. Reducing the number of points which defines an I_q Curve

For every I_q fixed value, 12 measurements for the d-axis currents have been considered. To obtain the minimum number of d-axis currents samples, a similar approach as in the previous section was applied. First, the problem size was reduced to half, through PCA. Secondly, a Ridge regression model was trained to predict the PCs I_d values (Table III).

Principal Component 0	91.0 A
Principal Component 1	113.0 A
Principal Component 2	110.0 A
Principal Component 3	110.0 A
Principal Component 4	110.0 A
Principal Component 5	110.0 A

TABLE III: Principal Components predicted values (I_d values)

The predicted values range is from 91 A to 113A, with the same value for the last four PCs. With this observation in mind, we can conclude that with the information obtained from the measurements of $I_d = 91A, I_d = 110A$ and $I_d = 113A$ we can reconstruct the entire family of I_q curves (with an 10^{-6} order error). Based on the obtained results, we can reduce to quarter the problem dimensions, with respect to OX axis.

V. INTERPOLATION FOR DIMENSIONALITY REDUCTION

A. Reducing the number of points which defines an I_q curve

In this section we will apply Polynomial Interpolation methods to find the minimum number of I_d measurements necessary to determine the characteristics of I_q curves.

First, we applied a cubic spline interpolation on the entire set of 12 points. Secondly, through an exhaustive search, we tried all possible combinations of lengths 10 up to 4, of the original set of points.

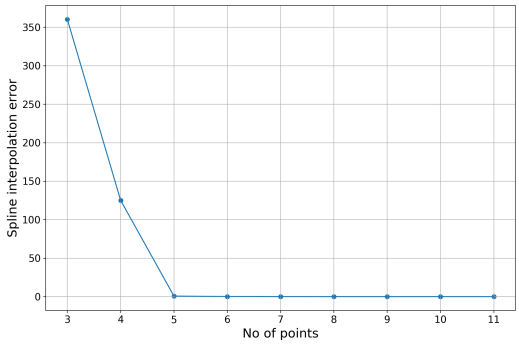

Fig. 5: Interpolation errors for different number of points

Based on the interpolation errors (see Fig. 5 and Fig 6), we can conclude that 5 points are enough to approximate the I_q characteristic as better as possible. For less than 5 points, the errors exceed the 10^2 order. This result allows us to reduce by half the measurements needed to obtain the d-axis magnetization characteristics of the studied machine.

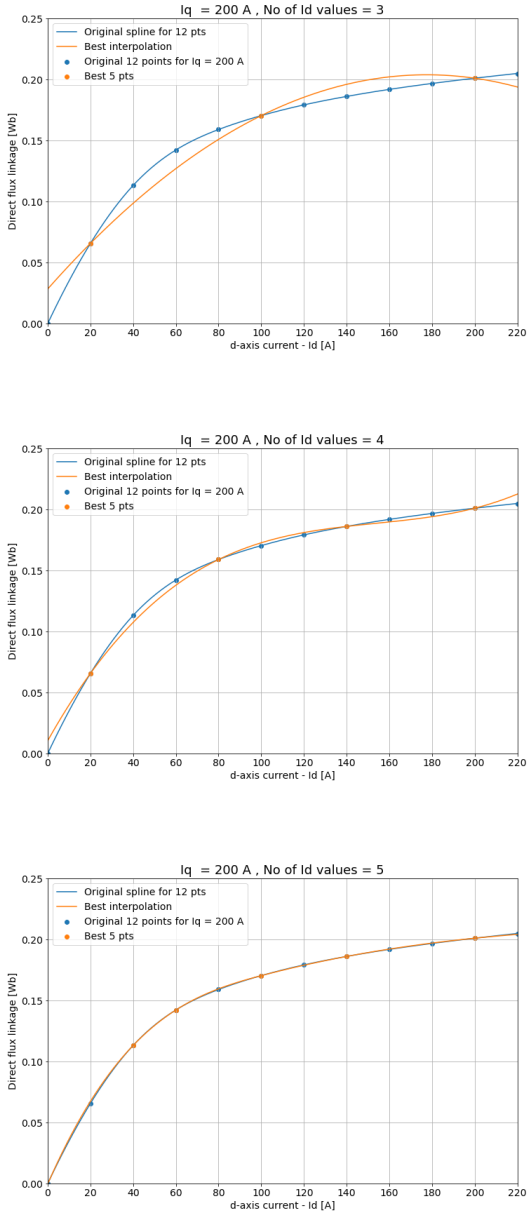

Fig. 6: Interpolation of $I_q = 200A$ for 3, 4 and 5 I_d values

B. *Reducing the number of Curves*

In this section interpolation is presented as a method to reduce the number of I_q curves necessary to describe the d-axis magnetization characteristics of the SynRM. In this approach, we fixed 2, 3, , 10 Iq curves, under the name of *generator curves*. Secondly, we reproduce the entire Iq family with the information contained in these generators. In each configuration, we chose the curves as evenly distributed as possible. For instance, we chose the first (I_q=0 A) and the last curve(I_q=220 A), for the 2 curves configuration; the first (I_q=0 A), the middle (I_q=100 A) and the last (II$_q$=220 A) curves, for the configuration with 3 curves, and so on and so forth. Those generators will be represented in black color (see Fig.8).

Let us consider the three curves configuration (I_q = 0 A, I_q = 100 A and I_q = 220 A) as an example to describe the process. First, each of the initial 12 curves is bordered by two generators (curve I_q = 80 A is between the first and the second generator, curve I_q = 140 A is between the second and the third generator, curve I_q=220 A is the third generator itself, and so on). Secondly, using the flux linkage matrix, the current curve flux is linearly interpolated, with respect to the borders' flux values. For an accurate result, all the 12 I_q curves, including the values corresponding to the generators, are interpolated.

The following equations define the interpolation formula used [23]:

$$\alpha = 1 - \frac{y - y_1}{y_2 - y_1}$$
$$y_{approx} = \alpha \cdot y_1 + (1 - \alpha) \cdot y_2 \tag{17}$$

where $y1$, y_2 - generators' flux linkage; x_1, x_2 - generators' d-axis currents (abscesses of each 5 best points); x - current curve abscesses of each 5 best points; y_{approx} - current curve flux linkage approximation.

From the previous section, it is a fact that 5 points are sufficient to describe an Iq curve. Being that said, for each Iq a set of 5 pairs (d-axis current value, direct flux linkage approximation) is considered. Through a cubic spline interpolation, every set of 5 points is bound in a curved line. The result represents the current curve approximation in the chosen configuration.

From Fig 7 we can conclude that the five curves configuration gives the best approximation of the I_q family of curves. In other words, with the measurements for I_q=0 A, I_q=40 A, I_q=100 A, I_q=160 A and I_q=220 A all the initial 12 I_q curves can be reproduced, with an 10^{-6} order error.

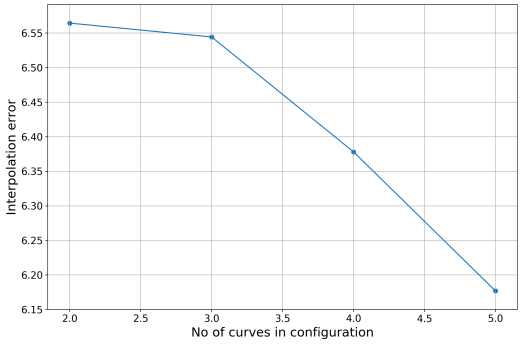

Fig. 7: Interpolation errors for different number of curves in configuration

For a visual understanding of the results, the curves corresponding to I_q=100 A and I_q=0 A values are represented in two different configurations (Fig.8).

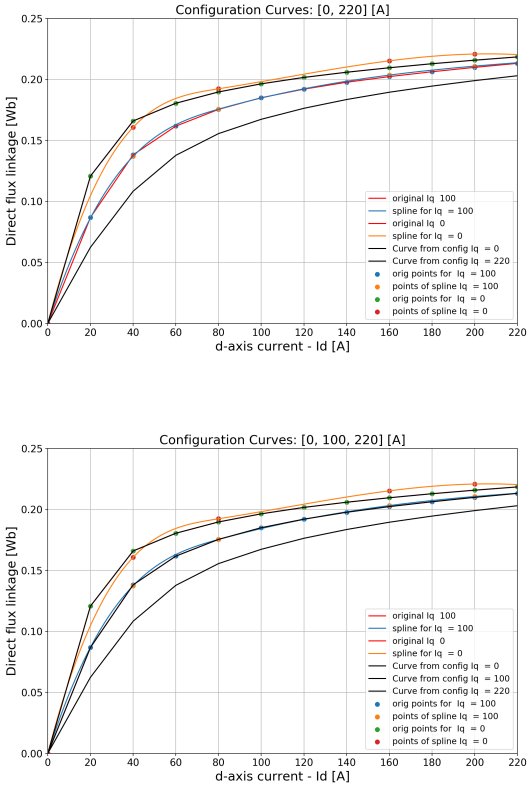

Fig. 8: Reconstructed curves

As a final interpretation, the polynomial interpolation approach results enable us to reduce the problem dimensionality to more than by half, with an 10^{-6} order error.

VI. Conclusion

The aim of this paper is to describe a method that covers interdisciplinary topics from electrical machines and machine learning, more particular, Model Order Reduction for Synchronous Reluctance Machine (SynRM)

We applied Principal Component Analysis, an unsupervised learning approach, widely used in machine learning fields, and two types of polynomial interpolation (linear and spline) to reduce the dimensions of the problem. The interpolation results were evaluated through least mean squared error. For the PCA approach, a Ridge regression model was trained to predict the values of the resulted principal components.

One of our future work interests is generalizing these methods to different types of electrical machines. Secondly, we intend to find and apply other machine learning techniques appropriate for the problem of dimensionality reduction.

References

[1] R. R. Moghaddam, "Synchronous reluctance machine (synrm) design," *Royal Institute of Technology (KTH)*, 2007.

[2] R.-R. Moghaddam and F. Gyllensten, "Novel high-performance synrm design method: An easy approach for a complicated rotor topology," *IEEE Transactions on Industrial Electronics*, vol. 61, no. 9, pp. 5058–5065, 2014.

[3] S. Tahi, R. Ibtiouen, and M. Bounekhla, "Design optimization of two synchronous reluctance machine structures with maximized torque and power factor," *Progress in Electromagnetics Research*, vol. 35, pp. 369–387, 2011.

[4] R. Rajabi Moghaddam, "Synchronous reluctance machine (synrm) in variable speed drives (vsd) applications," Ph.D. dissertation, KTH Royal Institute of Technology, 2011.

[5] M. Ferrari, N. Bianchi, A. Doria, and E. Fornasiero, "Design of synchronous reluctance motor for hybrid electric vehicles," *IEEE Transactions on Industry Applications*, vol. 51, no. 4, pp. 3030–3040, 2015.

[6] J. Ikaheimo, J. Kolehmainen, T. Kansakangas, V. Kivela, and R. R. Moghaddam, "Synchronous high-speed reluctance machine with novel rotor construction," *IEEE Transactions on Industrial Electronics*, vol. 61, no. 6, pp. 2969–2975, 2014.

[7] G. H. B. Foo and X. Zhang, "Robust direct torque control of synchronous reluctance motor drives in the field-weakening region," *IEEE Transactions on Power Electronics*, vol. 32, no. 2, pp. 1289–1298, 2017.

[8] ——, "Robust constant switching frequency-based field-weakening algorithm for direct torque controlled reluctance synchronous motors," *IEEE Transactions on Industrial Informatics*, vol. 12, no. 4, pp. 1462–1473, 2016.

[9] S. Ferdous, P. Garcia, M. A. M. Oninda, and M. A. Hoque, "Mtpa and field weakening control of synchronous reluctance motor," in *Electrical and Computer Engineering (ICECE), 2016 9th International Conference on*. IEEE, 2016, pp. 598–601.

[10] N. Bedetti, S. Calligaro, and R. Petrella, "Stand-still self-identification of flux characteristics for synchronous reluctance machines using novel saturation approximating function and multiple linear regression," *IEEE Transactions on Industry Applications*, vol. 52, no. 4, pp. 3083–3092, 2016.

[11] M. Degano, H. Mahmoud, N. Bianchi, and C. Gerada, "Synchronous reluctance machine analytical model optimization and validation through finite element analysis," in *Electrical Machines (ICEM), 2016 XXII International Conference on*. IEEE, 2016, pp. 585–591.

[12] S. E. Saarakkala, M. Sokolov, V. Mukherjee, J. Pippuri, K. Tammi, A. Belahcen, M. Hinkkanen *et al.*, "Flux-linkage model including cross-saturation for a bearingless synchronous reluctance motor," *Proc. ISMB15, Kitakyushu, Japan*, 2016.

[13] T. Herold, D. Franck, E. Lange, and K. Hameyer, "Extension of a dq model of a permanent magnet excited synchronous machine by including saturation, cross-coupling and slotting effects," in *Electric Machines & Drives Conference (IEMDC), 2011 IEEE International*. IEEE, 2011, pp. 1363–1367.

[14] K. J. Meessen, P. Thelin, J. Soulard, and E. Lomonova, "Inductance calculations of permanent-magnet synchronous machines including flux change and self-and cross-saturations," *IEEE transactions on magnetics*, vol. 44, no. 10, pp. 2324–2331, 2008.

[15] D. Yang, H. Mok, J. Lee, and S. Han, "Adaptive torque estimation for an ipmsm with cross-coupling and parameter variations," *Energies*, vol. 10, no. 2, p. 167, 2017.

[16] J. A. Lee and M. Verleysen, *Nonlinear dimensionality reduction*. Springer Science & Business Media, 2007.

[17] C. M. Bishop, *Pattern Recognition and Machine Learning*. Springer, 2006.

[18] M. E. Wall, A. Rechtsteiner, and L. M. Rocha, "Singular value decomposition and principal component analysis," in *A practical approach to microarray data analysis*. Springer, 2003, pp. 91–109.

[19] C. D. Meyer, *Matrix analysis and applied linear algebra*. Siam, 2000, vol. 71.

[20] G. Ottaviani and R. Paoletti, "A geometric perspective on the singular value decomposition," *arXiv preprint arXiv:1503.07054*, 2015.

[21] J. Shlens, "A tutorial on principal component analysis," *arXiv preprint arXiv:1404.1100*, 2014.

[22] P. Harrington, *Machine learning in action*. Manning Greenwich, CT, 2012, vol. 5.

[23] E. Cheney and D. Kincaid, *Numerical mathematics and computing*. Nelson Education, 2012.